analytical chemistry

ARTICLE

pubs.acs.org/ac

Positive Potential Operation of a Cathodic Electrogenerated Chemiluminescence Immunosensor Based on Luminol and Graphene for Cancer Biomarker Detection

Shoujiang Xu,[†,‡] Yang Liu,[*,†] Taihong Wang,[*,‡] and Jinghong Li[*,†]

[†]Key Lab of Bioorganic Phosphorus Chemistry and Chemical Biology, Department of Chemistry, Tsinghua University, Beijing 100084, China

[‡]College of Materials Science and Engineering, and Key Laboratory for Micro−Nano Optoelectronic Devices of Ministry of Education, Hunan University, Changsha 410082, China

Supporting Information

ABSTRACT: In this work, we report a cathodic electrogenerated chemiluminescence (ECL) of luminol at a positive potential (ca. 0.05 V vs Ag/AgCl) with a strong light emission on the graphene-modified glass carbon electrode. The resulted graphene-modified electrode offers an excellent platform for high-performance biosensing applications. On the basis of the cathodic ECL signal of luminol on the graphene-modified electrode, an ECL sandwich immunosensor for sensitive detection of cancer biomarkers at low potential was developed with a multiple signal amplification strategy from functionalized graphene and gold nanorods multilabeled with glucose oxidase (GOx) and secondary antibody (Ab_2). The functionalized graphene improved the electron transfer on the electrode interface and was employed to attach the primary antibody (Ab_1) due to it large surface area. The gold nanorods were not only used as carriers of secondary antibody (Ab_2) and GOx but also catalyzed the ECL reaction of luminol, which further amplified the ECL signal of luminol in the presence of glucose and oxygen. The as-proposed low-potential ECL immunosensor exhibited high sensitivity and specificity on the detection of prostate protein antigen (PSA), a biomarker of prostate cancer that was used as a model. A linear relationship between ECL signals and the concentrations of PSA was obtained in the range from 10 pg mL^{-1} to 8 ng mL^{-1}. The detection limit of PSA was 8 pg mL^{-1} (signal-to-noise ratio of 3). Moreover, the as-proposed low-potential ECL immunosensor exhibited excellent stability and reproducibility. The graphene-based ECL immunosensor accurately detected PSA concentration in 10 human serum samples from patients demonstrated by excellent correlations with standard chemiluminescence immunoassay. The results suggest that the as-proposed graphene ECL immunosensor will be promising in the point-of-care diagnostics application of clinical screening of cancer biomarkers.

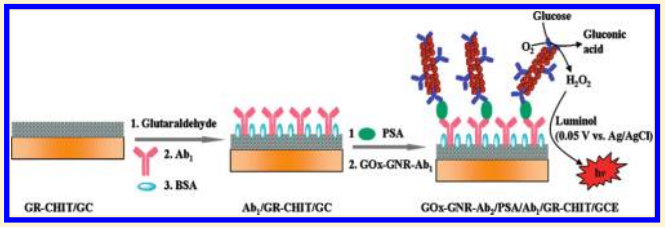

The increasing demands of diseases diagnostics and therapeutic analysis require the development of sensitive and accurate detection of disease-related proteins. In particular, the clinical analysis of cancer biomarker is critical to the early cancer diagnostic and proteomics research, which will also promote the understanding of cancer diseases' related biological processes.[1−3] Immunoassay based on the highly specific interaction between antigen and antibody is one of the most important methods for the specific analysis of those cancer biomarkers. Until now, several immunoassay methods including radioimmunoassay,[4] fluorescence immunoassay,[5,6] enzyme-linked immunosorbent assay (ELISA),[7] chemiluminescence immunoassay,[8,9] mass spectrometric immunoassay,[10,11] electrophoretic immunoassay,[12] and immune polymerase chain reaction (PCR) assay[13] have been conducted on the clinical serum sample measurements. However, it is still a critical demand on simple, rapid, sensitive, and low-cost detection technologies for the earlier and sensitive profiling of cancer biomarkers, especially in the point-of-care applications.

Electrogenerated chemiluminescence (ECL), involving a light emission process in a redox reaction of electrogenerated reactants, combines the electrochemical and luminescent techniques.[14−17] In comparison to the conventional electrochemical methods, the ECL assay not only shows high sensitivity and wide dynamic concentration response range but also is potential- and spatial-controlled. By integrating the high affinity of antigen−antibody, the ECL immunoassay has become a powerful analytical tool for highly sensitive and specific detection of clinical samples.[18−20]

The rapid developments of nanostructure materials promote the evolution of high-performance ECL immunosensors due to their good biocompatibility, fascinating electrocatalytic activity, large surface area, excellent conductivity, and so on. The nanoparticles can work as a promoter to increase the surface area and improve the electron transfer at the electrode interface. They can

Received: February 3, 2011
Accepted: April 12, 2011
Published: April 22, 2011

Scheme 1. (A) Modification Procedure of Gold Nanorods and (B) ECL Immunoassay of PSA with Multiple Amplification Strategy Based on a Graphene Composite Modified Electrode

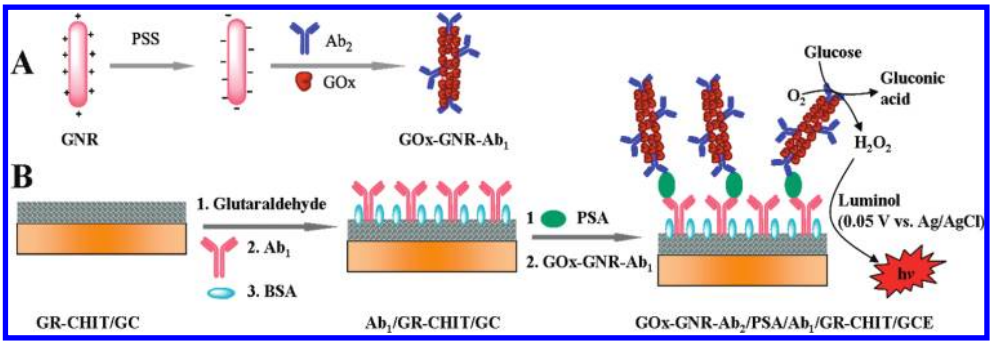

also be used as carriers to load a large amount of ECL labels and biomolecules and thus afford substantial ECL signal amplification and the enhancement of performances of the biosensors.[21−26] For example, Rusling's group achieved enhanced sensitivity using a single-wall carbon nanotube forest modified electrode with silica nanoparticles loaded with $Ru(bpy)_3^{2+}$ and secondary antibody for the ECL immunoassay of prostate-specific antigen (PSA).[27] Cui's group gained a great enhancement on the sensitivity of the ECL immunosensor using luminol-conjugated gold nanoparticles.[28] Great improvements on the performances of the ECL biosensor based on quantum dots were also realized based on carbon nanotubes, gold nanoparticles, and so on.[19,23,25]

Recently, much attention has been centered on graphene due to its fascinating two-dimensional structure, unusual electrochemical properties, large accessible surface area, as well as good biocompatibility.[29−34] Graphene presents excellent electron-transfer ability for some enzymes[35,36] and excellent catalytic behavior toward small molecules[37−42] such as dopamine, H_2O_2, O_2, NADH, and TNT. In addition, the large surface area of graphene and related derivates also allows it to be an excellent carrier to load more active probes and active domains for biomolecules binding, offering a significant amplification on the electrochemical sensing signals.[43−45] In addition, graphene oxide also exhibited ECL behavior at a potential of 1.15 V versus SCE (saturated calomel electrode).[46] Besides its intrinsic ECL behavior, improved ECL performance was also achieved on the graphene or its derivates modified electrodes.[47−50] It has been reported that improved ECL intensity of quantum dots was obtained in the presence of graphene oxide.[51] The unique properties of graphene allow it to be an excellent platform for biosensor construction.

In this work, the cathodic ECL behavior of luminol at a positive potential on a graphene-modified electrode is reported. On the basis of the strong and stable cathodic ECL signal, an ECL sandwich immunosensor for sensitive detection of cancer biomarkers was proposed with a multiple signal amplification strategy from functionalized graphene and enzyme−antibody-conjugated gold nanorods as the sensor platform as shown in Scheme 1. The as-synthesized gold nanorods were serviced as carriers to load more secondary antibodies (Ab_2) and glucose oxidase (GOx). The chitosan-functionalized graphene-modified glassy carbon (GC) electrode was employed to increase the loading of primary antibody (Ab_1) and catalyzed the cathodic ECL reaction which was further amplified by the gold nanorods and the enzyme-catalyzed reaction. Here, prostate protein antigen (PSA), a biomarker for prostate cancer,[52] was used as a model cancer marker and illustrated the amplification process in the sandwich ECL detection. The results were also correlated with standard chemiluminescence immunoassay. The as-proposed ECL immunosensor based on graphene shows great promise in the point-of-care diagnostics application of clinical screening of cancer biomarkers.

EXPERIMENTAL SECTION

Materials and Reagents. Graphite powder (99.99995%, 325 mesh) was purchased from Alfa Aesar. Two mouse antihuman total PSA monoclonal antibodies, clone P27A10 (primary capture antibody (Ab_1)) and clone P27B1 (secondary detection antibody (Ab_2)) were gotten from Shuangliu Zhenglong Biochemical Lab (Chengdu, China). Total prostate-specific antigen, fetoprotein (AFP), human thyroglobulin (hTG), and carcinoembryonic antigen (CEA) were received from National Institute for Control of Pharmaceutical and Biological Products. Clinical serum samples of PSA with different concentrations were provided by the Affiliated Hospital of Tsinghua University. Human serum albumins (HSA), bovine serum albumin (BSA), and human immunoglobulin G (hIgG) were from Dingguo Biological Products Company (Beijing, China). Glucose oxidase (GOx, 100−250 units/mg), chitosan (CHIT: MW ca. 1×10^6, >85% deacetylation), luminol, Tween-20, and glutaraldehyde were purchased from Sigma. $HAuCl_4 \cdot 3H_2O$ (48% w/w) was obtained from Shanghai Reagent (Shanghai, China). A 1.0×10^{-2} M stock solution of luminol was prepared by dissolving luminol in 0.1 mol/L sodium hydroxide solution. Phosphate buffer solutions (PBS) were prepared with $Na_2HPO_4 \cdot 12H_2O$ and $NaH_2PO_4 \cdot 2H_2O$, and the PBS (pH 7.4, 10 mM) solution containing 145 mM NaCl and 0.05% (w/v) Tween 20 was used as washing solution. Other regents of analytical grade were obtained from Beijing Chemical Company (China) and were used as received.

The graphene was synthesized according to our previous works.[41,42] The preparation of gold nanorods (GNRs) was reported elsewhere.[53−55] The detail information of the preparation of graphene, gold nanorods, and Ab_2- and GOx-conjugated gold nanorods (GOx−GNR−Ab_2) is shown in the Supporting Information. The characterization of final graphene, GNRs, and Ab_2- and GOx-conjugated gold nanorods (GOx−GNR−Ab_2, Scheme 1A) is shown in Figure 1S and Figure 2S in the Supporting Information, respectively.

Fabrication of ECL Immunosensors. Prior to fabrication of immunosensors, a GC electrode (diameter of 3 mm) was

dx.doi.org/10.1021/ac200237j |Anal. Chem. 2011, 83, 3817–3823

successively polished with 1.0, 0.3, and 0.05 μm α-Al_2O_3 powder and ultrasonically cleaned with ethanol and water. An amount of 1 mg of as-synthesized graphene was dispersed in 1 mL of 0.2% chitosan solution to get a homogeneous suspension by sonication. The graphene−chitosan-modified GC electrode (GR−CHIT/GC) was prepared by casting 10 μL of the suspension on the surface of the GC electrode and drying at room temperature. For the immobilization of Ab_1, the above GR−CHIT/GC electrode was immersed in a 2.5% glutaric dialdehyde solution for about 1 h. After washing, 20 μL of 200 μg mL^{-1} Ab_1 was dropped onto the electrode surface, allowing it to react for 1 h at 37 °C to get the Ab_1-immobilized GR−CHIT/GC (Ab_1/GR−CHIT/GC). Then, the washed Ab_1/GR−CHIT/GCE was incubated in 3% BSA for 30 min at 37 °C to block the excess active groups on the surface, followed by washing, and used for the PSA detection.

Procedure for Detection of PSA. A sandwich immunoassay was conducted for the detection of PSA antigen. The immunosensor, Ab_1/GR−CHIT/GC, was first incubated with 20 μL of PSA standard antigen solutions at different concentrations, followed by washing thoroughly with washing buffer. Second, the electrode of PSA/Ab_1/GR/GCE was further incubated with 20 μL of colloidal solution of GOx−GNR−Ab_2 for 1 h at 37 °C, followed by the similar washing steps as above. The ECL immunoassay was then conducted in a PBS solution with 100 μM luminol and 10 mM glucose. A Ag/AgCl electrode with saturated KCl solution and platinum wire were used as the reference electrode and counter electrode, respectively, in all ECL measurements. The measurement of clinical serum samples was performed with the same procedures mentioned above without any other treatments.

Characterization. Transmission electron microscope (TEM) images were obtained with a JEM-2010 high-resolution TEM system (JEOL, Japan) opened at an accelerating voltage of 200 kV. The scanning electron microscopy (SEM) image was obtained using a JSM-7401 field emission SEM system (JEOL, Japan). X-ray diffraction (XRD) patterns were obtained using a D8 Advance (Bruker) X-ray diffractometer with Cu Kα radiation (λ = 1.5418 Å). Raman spectra were obtained using a confocal microprobe Raman system (Renishaw, RM2000). UV−vis experiments were performed with a UV-3900 spectrophotometer (Hitachi, Japan).

The cyclic voltammetry was conducted on a CHI 660b instrument (CH Instrument Co.). Electrochemical impedance spectroscopy (EIS) was carried out on a PARSTAT 2273 potentiostat/galvanostat (Advanced Measurement Technology Inc.). Impedance measurements were performed by applying an ac voltage of 5 mV amplitude in the 0.01 Hz to 10^5 Hz frequency range in a 5 mM $K_3[Fe(CN)_6]/K_4[Fe(CN)_6]$ redox probe solution with 0.1 M KCl. The ECL measurements were carried out on an MPI-B multifunctional electrochemical analytical system (Xi'an Remex Analytical Instrument Ltd. Co., China). If no special statements are made, the voltage of the PMT was maintained at 500 V.

RESULTS AND DISCUSSION

ECL of Luminol on Graphene-Modified Electrodes. The anodic ECL responses of luminol have been variously studied on the nanomaterial-modified electrodes, and the enhanced anodic ECL signal was also reported on a graphene/Nafion-modified GC electrode.[47] However, little attention has been paid to the cathodic ECL behavior of luminol and its biosensing application. Here, the ECL behavior of luminol on a GR−CHIT/GC electrode was studied in a PBS solution (pH 7.6). As shown in Figure 1A, an anodic ECL peak at ca. 0.5 V was obtained (curve b) and the ECL response on the GR−CHIT/GC electrode was obviously larger than that on bare GC electrode (curve a), which was similar to that reported.[47] The enhancement of ECL intensity would be attributed to the large surface area and excellent electron-transfer performance of graphene. Besides the anodic ECL peak, it was noted that a strong cathodic ECL peak was also observed at ca. 0.1 V. As a comparison, nearly no ECL response was obtained at a bare GC electrode in the potential range. To verify the ECL peak, the chemiluminescence of the cathodic and anodic ECL responses was measured (Figure S3 in the Supporting Information). Like that of the anodic ECL response of luminol on the bare GC electrode in alkaline solution (pH 10.5), both the cathodic and anodic ECL responses on the graphene-modified electrode were centered at 460 nm, corresponding to the light emission of 3-aminophthalate.[56] The wavelength shift of luminol emission would be attributed to the environmental change during the luminol ECL reaction.[56] In addition, the ECL behavior of luminol on the graphene oxide−chitosan-modified GC electrode prepared in the same manner was also studied. Like that of the bare GC electrode, no obvious ECL response was observed (Figure S4 in the Supporting Information). Moreover, the similar results were also

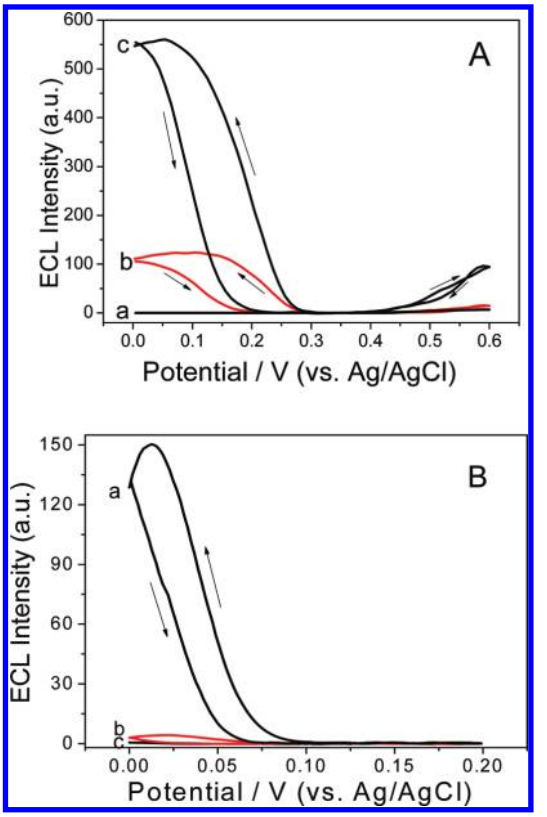

Figure 1. (A) ECL−potential curves of the bare GC electrode (curve a) in PBS solution (pH 7.6) containing 100 μM luminol, and the ECL−potential curves of the GR−CHIT/GC electrode in PBS solution (pH 7.6) containing 100 μM luminol before (curve b) and after (curve c) the addition of 10 μM H_2O_2. (B) The cathodic ECL response of the GR−CHIT/GC electrode in the PBS solution (pH 7.6) containing 100 μM luminol before (curve a) and after (curve b) being saturated with nitrogen and that performed in the electrolyte containing 35 U of SOD without deaeration (curve c).

obtained when the ECL measurements of the graphene−chitosan-modified electrodes were conducted by using a salt-bridge system to separate the working and counter electrodes (Figure S5A in the Supporting Information). The facts indicated that graphene played an important role on the cathodic ECL behavior of luminol on the surface of the GR−CHIT/GC electrode. The cathodic ECL behavior of luminol is generally ascribed to the generation of reactive oxygen species such as superoxide radical and hydrogen peroxide in the electrolyte[57,58] on surface of the electrode, which reacts with luminol to produce excited 3-aminophthalate dianion and finally emits lights. To verify the roles of reactive oxygen species in the cathodic ECL behavior, Figure 1B presents the cathodic ECL response of the GR−CHIT/GC electrode in the luminol solution before (curve a) and after (curve b) being saturated with nitrogen. It was clear that the cathodic ECL response of luminol decreased significantly and nearly no ECL peak was observed in the nitrogen-saturated solution. In addition, superoxide dismutase (SOD), a typical $O_2^{\bullet-}$ capture, was added into the air-saturated solution to test the effect of $O_2^{\bullet-}$. As shown in Figure 1B (curve c), the cathodic ECL signal showed a dramatic decrease in the presence of SOD. In addition, the influence of H_2O_2 on the ECL behavior of luminol on the graphene−chitosan-modified GC electrode is also shown in Figure 1A (curve c). Both the cathodic and anodic ECL peaks of luminol on the GR−CHIT/GC electrode improved intensively, which was similar to those reported.[57,58] These results suggested that reactive oxygen species, such as superoxide anion and hydroxyl radical, etc., were critical on the cathodic ECL behavior of luminol on the GR−CHIT/GC electrodes. As a result, we propose that the cathodic ECL response of luminol can be ascribed to the excellent electrocatalytic properties of graphene that facilitate the reduction of O_2 in a solution dissolved with trace oxygen, although no obvious redox peak was observed (Figure S5B in the Supporting Information). The generated reactive oxygen species such as $O_2^{\bullet-}$ and H_2O_2 would further oxidize luminol to produce 3-aminophthalate, and finally light emission took place. In the experiments, we found that both the cathodic and anodic ECL responses on the GR−CHIT/GC electrode presented excellent stability as shown in Figure S6 in the Supporting Information. Moreover, the cathodic ECL response is extremely larger than that of the anodic ECL peak, which implies that a highly sensitive ECL sensor can be gained based on the cathodic ECL behavior of luminol at such a low potential on the graphene-modified GC electrode.

Multiple Signal Amplification Strategy for ECL Immunosensors Using Graphene and GOx−GNR−Ab_2. Scheme 1B reveals the ECL immunoassay steps with multiamplification strategy. Here, the graphene sheets are not only used to electrocatalyze the ECL process of luminol but also acted as a sensor platform to increase the surface area that captures a mass of Ab_1. Moreover, owing to its excellent electron-transfer ability, the graphene also improved the electron transfer at the electrode interface, thus improving the sensitivity of the as-designed ECL immunosensor. Ab_2 and GOx serve as the probing antibody and the enzymic ECL signal-amplifying agent in a sandwiched immunoassay, respectively, which are loaded on gold nanorods to increase the quantities of both enzyme and probe antibodies. Moreover, the gold nanorod itself can also improve the ECL reaction of luminol, thus enhancing the sensitivity of the immunosensor.

ECL Behaviors of the Immunosensors. The ECL behaviors of the immunosensor were characterized step by step in 0.1 M PBS (pH 7.6) containing 100 μM luminol. As shown in Figure 2, the GC electrode did not show any detectable signal at such a low potential (curve a). After the modification, electrode exhibited a stable ECL signal at 0.05 V resulting from the ECL reaction of luminol as described before. The ECL signal decreased quickly upon the conjugation of Ab_1 and BSA on the electrode due to the electron-transfer inhibition on the electrode interface by the inert biomolecules (curve c). The ECL intensity of the Ab_1/GR−CHIT/GC electrode decreased further after incubating it in the solution of PSA. Wherever, when we immersed the PSA/Ab_1/GR−CHIT/GC electrode into the colloidal solution of GOx−GNR−Ab_2, a strong ECL peak was observed at the same potential (curve e). The emission intensity of luminol after the assembly of gold nanorods was nearly 10 times larger than that before incubation. The enhancement of the ECL signal of luminol could be ascribed to the excellent electron-transport ability of gold nanorods, which is similar to the CV and EIS results (Figure S7 in the Supporting Information). In addition, it has been reported that gold nanorods also exhibit excellent electrocatalytic performance to the ECL reaction of luminol.[58] In order to verify the enzymic amplification of the immunosensor, the ECL behavior of the GOx−GNR−Ab_2/PSA/Ab_1/GR−CHIT/GC electrode was studied by adding 10 mM glucose into the above luminol solution. As shown, the ECL signal of luminol showed a sharp increase (curve f). The intense ECL signal was originated from the GOx-mediated electrooxidation of glucose in the presence of oxygen that yielded gluconic acid and hydrogen peroxide. Then the in situ produced hydrogen peroxide reacted with luminol, and the multiple enzymatic turnovers significantly amplified the generated ECL photons. The controlled experiments were also conducted by measuring the ECL intensity of the Ab_1/GR−CHIT/GC electrode without the treatment of PSA followed by incubating the electrode in the colloidal solution of GOx−GNR−Ab_2. As shown in the inset of Figure 2, the Ab_1/GR−CHIT/GC electrode without the treatment of PSA exhibited a much smaller signal in the PBS solution containing both luminol and glucose (the inset of Figure 2,

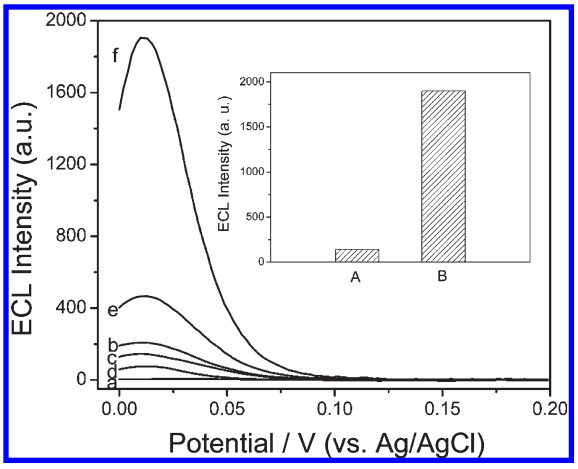

Figure 2. ECL−potential curves of the bare GC electrode (a), GR−CHIT/GCE (b), Ab_1/GR−CHIT/GCE (c), PSA/Ab_1/GR−CHIT/GCE (d), and GOx−GNR−Ab_2/PSA/Ab_1/GR−CHIT/GCE (without (curve e) and with (curve f) 10 mM glucose) in 0.1 M PBS solution (pH 7.6) containing 100 μM luminol. Scan rate, 100 mV s^{-1}. The voltage of the PMT was maintained at 500 V. The inset shows the ECL intensity of the Ab_1/GR−CHIT/GCE (A) and GOx−GNR−Ab_2/PSA/Ab_1/GR−CHIT/GCE electrodes (B) at 0.05 V vs Ag/AgCl.

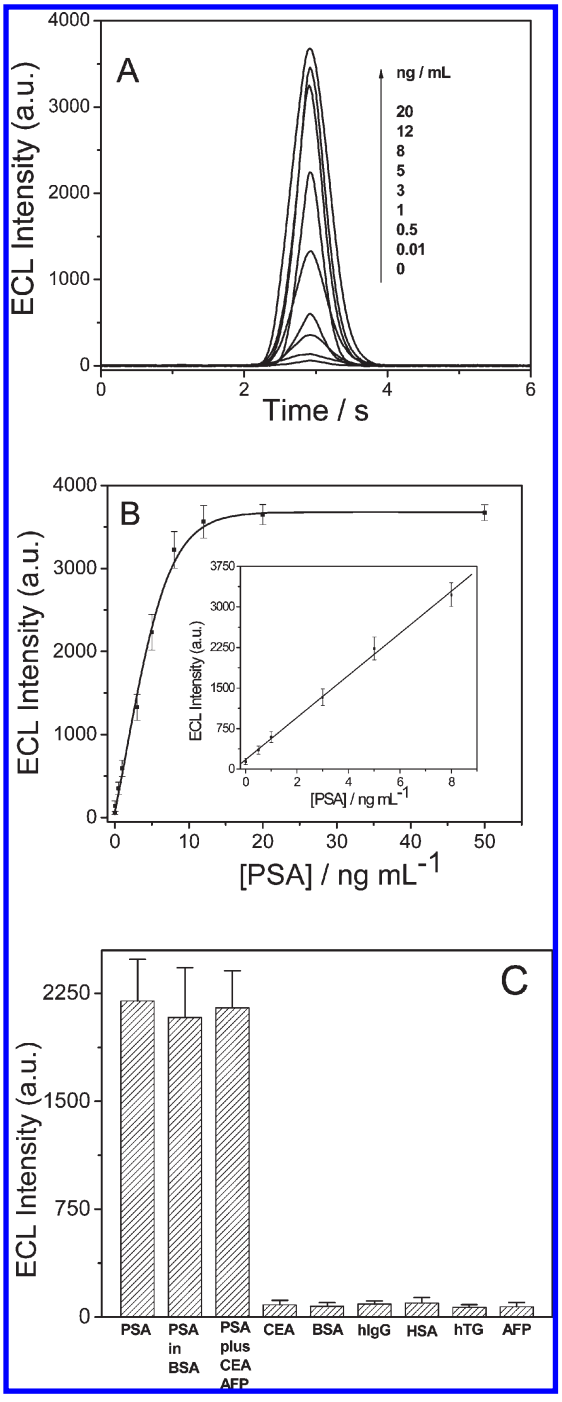

Figure 3. (A) ECL profiles of the GOx−GNR−Ab_2/PSA/Ab_1/GR−CHIT/GCE immunosensors in the presence of different concentrations of PSA in 0.1 M PBS solution (pH 7.6) containing 100 μM luminol and 10 mM glucose. (B) The dependence of ECL intensity on the concentration of PSA. Inset: the linear relationship between the ECL intensity at 0.05 V vs Ag/AgCl and the PSA concentrations. (C) The ECL responses at 0.05 V vs Ag/AgCl of the immunosensor to 5 ng/mL PSA in the absence (PSA) and the presence of 10% BSA solution (PSA in BSA), 500 μg/mL CEA and 500 μg/mL AFP (PSA plus CET AFP), respectively, and the ECL responses of the immunosensor to 1 mg/mL CEA (CEA), 1 mg/mL BSA (BSA), 1 mg/mL human IgG (hIgG), 1 mg/mL HAS (HAS), 1 mg/mL hTG (Htg), and 500 μg/mL AFP (AFP). Error bars were obtained from three times parallel experiments.

column A) than that of the PSA/Ab_1/GR−CHIT/GC electrode (column B).

Optimization of Detection Condition. The immunoreaction time is an important parameter for the PSA capture and the specific recognition of GOx−GNR−Ab_2 on the electrode. By increasing the immunoreaction time, the ECL signal increased and reached a plateau after 60 min (Figure S9A in the Supporting Information), indicating a tendency to complete immunoreaction on the electrode surface. Therefore, the optimal immunoreaction time was 60 min.

The sensitivity of the proposed immunosensor is relied on the formation of the immunocomplex on the electrode which is dependent on the amount of GOx and Ab_2 conjugated on the gold nanorods. More GOx molecules on the gold nanorods will improve the reaction to generate more H_2O_2 and enhances the ECL intensity. However, an excessive amount of GOx will also reduce the quantity of Ab_2 and weaken the binding between gold nanorods and electrode surface. To obtain the best performance of the immunosensor, gold nanorods modified with GOx and Ab_2 at different mass ratios were synthesized and used for the construction of the immunocomplex (Figure S9B in the Supporting Information). As shown, the maximal ECL signal was achieved at a mass ratio of GOx to Ab_2 of 300. Thus, the functionalized gold nanorod synthesized in the solution with a mass ratio of GOx to Ab_2 of 300 was employed in the modification of gold nanorods for the following immunosensors construction.

ECL Detection of PSA. On the basis of the optimal condition, the sandwiched immunoassay was applied for the PSA detection. When the PSA concentration increased, the ECL signal of GOx−GNR−Ab_2/PSA/Ab_1/GR−CHIT/GCE increased accordingly (Figure 3A) and reached a saturation value once the concentration of PSA was above 20 ng mL^{-1}. The dependence of the ECL response on the PSA concentration is presented in Figure 3B. A linear relationship between ECL signals and the concentrations of PSA was obtained in the range from 10 pg mL^{-1} to 8 ng mL^{-1}. The detection limit of PSA was 8 pg mL^{-1} (signal-to-noise ratio of 3), which was lower than that of 40 pg mL^{-1} PSA on the ECL immunoassays based on a carbon nanotube forest and dye-doped silica sphere.[56] The linear relationship can be represented as $I = 174.9 + 389.4c$ with the correlation coefficient of $R^2 = 0.9967$, where I is the ECL intensity and c is the PSA concentration. Generally, the concentration of PSA in human serum at 4−10 ng mL^{-1} is a indicative of prostate cancer, and the normal levels of PSA are below 3 ng mL^{-1}. This demonstrates that the proposed ECL immunosensor can be employed for highly sensitive PSA detection in clinical human serum samples without any treatments.

To further verify the selectivity of the proposed immunosensors for PSA detection, the as-prepared immunosensor was incubated in the PSA solution containing different interfering agents, such as AFP and CEA. The results are shown in Figure 3C. No remarkable change of ECL signal was observed as compared to that of PSA only. On the other hand, much weak ECL signal was observed by replacing PSA with hIgG, AFP, CEA in the solution, showing the excellent selectivity of the as-proposed PSA ECL immunosensor.

Evaluation of the ECL Immunosensor. A low operation potential can avoid the damage of the modified electrodes and biomolecules, supplying a high stability of the ECL biosensor for PSA detection. Figure 4 shows the ECL response of the immunosensor with successive scanning. Stable and high ECL signals were observed, which signified that the ECL biosensor

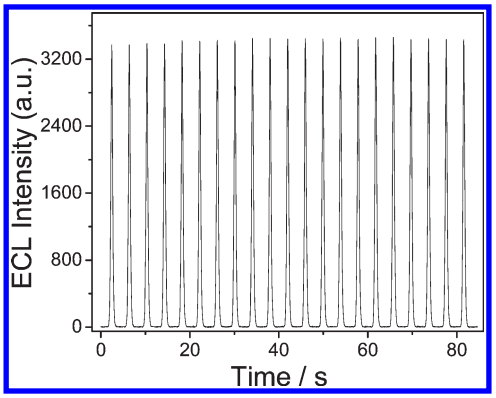

Figure 4. ECL−time curve of the ECL immunosensor at a PSA concentration of 10 ng/mL under continuous cyclic voltammetry scan with a scan rate of 100 mV s^{-1}. All experiments were carried out in 0.1 M PBS solution (pH 7.6) containing 100 μM luminol and 10 mM glucose. The potential range of the scan was 0−0.2 V.

Table 1. Comparison of the Graphene-Based Electrogenerated Chemiluminescence (ECL) Immunosensor with Chemiluminescence (CL) Immunoassay for Clinical PSA Detection

clinical serum sample	ECL, ng/mL	CL, ng/mL	relative difference, %
1	0.112(0.008)	0.103	8.74
2	0.362 (0.037)	0.349	3.72
3	0.710(0.021)	0.678	4.72
4	1.144(0.043)	1.124	1.82
5	1.455(0.036)	1.384	5.11
6	2.030(0.019)	2.064	−1.65
7	2.485(0.023)	2.305	7.83
8	2.537(0.062)	2.810	−9.71
9	4.072(0.043)	3.766	8.13
10	5.846(0.038)	5.614	4.79

possessed excellent potential cycling stability. The reproducibility of the ECL biosensor was also investigated with intra- and interassay precision. The intraassay precision of the ECL biosensor was evaluated by measuring the PSA with concentration of 10 ng mL^{-1} for 10 times. The interassay precision was assessed by assaying the PSA at the same concentration for 10 electrodes. The intra- and the interassay variation coefficients obtained from 10 ng mL^{-1} were 5.47% and 6.16%, respectively. Both the intra- and interassays of the as-designed ECL biosensor enunciated good reproducibility.

To demonstrate the potential of the as-proposed ECL immunosensor in clinical application, 10 human serum samples from patients with prostate diseases were measured by using the graphene-based ECL immunosensors and were compared to a chemiluminescence immunoassay. Table 1 presents the estimated concentrations of PSA in these samples with both methods. It was shown that the as-prepared graphene-based ECL immunosensor displayed a deviation ranging from −9.71% to 8.74% from those obtained with chemiluminescence. These results illustrated that the as-prepared graphene-based ECL immunosensor was comparable to the clinical assay, exhibiting great promise as a reliable technique for the detection of PSA in serum samples.

CONCLUSIONS

In conclusion, a cathodic ECL response of luminol at a positive potential with a strong light emission on a graphene-modified glassy carbon electrode was observed, which would be attributed to the facilitated generation of reactive oxygen species, such as superoxide anion and hydroxyl radical, etc., on the graphene. The unique ECL performances on the graphene-modified electrode offer it to be an excellent sensing platform. On the basis of the strong and stable cathodic ECL signal of luminol on the graphene-modified electrode, a sandwich ECL immunosensor for sensitive detection of cancer biomarkers was successfully developed with a multiple signal amplification strategy from functionalized graphene and gold nanorods multilabeled with GOx and Ab_2. The as-proposed ECL immunosensor exhibited excellent performances, such as low operation potential, high sensitivity and selectivity, etc., on the detection of prostate protein antigen in clinical human serum samples. The ECL immunosensor can also be extended for the detection of other relative biomarkers, which shows great potential in point-of-care applications for accurate clinical diseases diagnostic.

ASSOCIATED CONTENT

Supporting Information. Additional information as noted in text. This material is available free of charge via the Internet at http://pubs.acs.org.

AUTHOR INFORMATION

Corresponding Author

*Phone: 86-10-62795290. Fax: 86-10-62771149. E-mail: liu-yang@mail.tsinghua.edu.cn (Y.L.); jhli@mail.tsinghua.edu.cn (J.L.); thwang@hnu.cn (T.W.).

ACKNOWLEDGMENT

This work was financially supported by the National Natural Science Foundation of China (Nos. 20975060, 21005046), National Basic Research Program of China (Nos. 2007CB310500, 2011CB935700), European Commission Specific Programme GlycoHIT (FP7-HEALTH-2010, No. 260600), and Tsinghua University Initiative Scientific Research Program. We thank Jinsheng Cheng for the synthesis of graphene in the experiments.

REFERENCES

(1) Xiao, Z.; Prieto, D.; Conrads, T. P.; Veenstra, T. D.; Issaq, H. J. *Mol. Cell. Endocrinol.* **2005**, *230*, 95–106.
(2) Weston, A. D.; Hood, L. *J. Proteome Res.* **2004**, *3*, 179–196.
(3) Kitano, H. *Science* **2002**, *295*, 1662–1664.
(4) Goldsmith, S. J. *Semin. Nucl. Med.* **1975**, *5*, 125–152.
(5) Matsuya, T.; Tashiro, S.; Hoshino, N.; Shibata, N.; Nagasaki, Y.; Kataoka, K. *Anal. Chem.* **2003**, *75*, 6124–6132.
(6) Cesaro-Tadic, S.; Dernick, G.; Juncker, D.; Buurman, G.; Kropshofer, H.; Michel, B.; Fattinger, C.; Delamarche, E. *Lab Chip* **2004**, *4*, 563–569.
(7) Yates, A. M.; Elvin, S. J.; Williamson, D. E. *J. Immunoassay* **1999**, *20*, 31–44.
(8) Fu, Z.; Hao, C.; Fei, X.; Ju, H. *J. Immunol. Methods* **2006**, *312*, 61–67.
(9) Voller, A.; Bartlett, A.; Bidwell, D. E. *J. Clin. Pathol.* **1978**, *31*, 507–520.
(10) Hu, S.; Zhang, S.; Hu, Z.; Xing, Z.; Zhang, X. *Anal. Chem.* **2007**, *79*, 923–929.
(11) Aebersold, R.; Mann, M. *Nature* **2003**, *422*, 198–207.

(12) Schmalzing, D.; Nashabeh, W. *Electrophoresis* **1997**, *18*, 2184–2193.
(13) Saito, K.; Kobayashi, D.; Sasaki, M.; Araake, H.; Kida, T.; Yagihashi, A.; Yajima, T.; Kameshima, H.; Watanabe, N. *Clin. Chem.* **1999**, *45*, 665–669.
(14) Bard, A. J. *Electrogenerated Chemiluminescence*; Marcel Dekker: New York, 2004.
(15) Richter, M. M. *Chem. Rev.* **2004**, *104*, 3003–3036.
(16) Marquette, C. A.; Blum, L. J. *Anal. Bioanal. Chem.* **2009**, *390*, 155–168.
(17) Bertoncello, P.; Forster, R. J. *Biosens. Bioelectron.* **2009**, *24*, 3191–3200.
(18) Ala-Kleme, T.; Makinen, P.; Ylinen, T.; Vare, L.; Kulmala, S.; Ihalainen, P.; Peltonen, J.-cite-author>Anal. Chem. 2006, 78, 8288.
(19) Liu, X.; Ju, H. X. *Anal. Chem.* **2008**, *80*, 5377–5382.
(20) Miao, W.; Bard, A. J. *Anal. Chem.* **2004**, *76*, 7109–7113.
(21) Duan, R.; Zhou, X.; Xing, D. *Anal. Chem.* 2010, *82*, 3099–3103.
(22) Pinijsuwan, S.; Rijiravanich, P.; Somasundrum, M.; Surareungchai, W. *Anal. Chem.* **2008**, *80*, 6779–6784.
(23) Jie, G.; Zhang, J.; Wang, D.; Cheng, C.; Chen, H. Y.; Zhu, J. J. *Anal. Chem.* **2008**, *80*, 4033–4039.
(24) Duan, R.; Zhou, X.; Xing, D. *Anal. Chem.* **2010**, *82*, 3099–3103.
(25) Jie, G. F.; Liu, P.; Wang, L.; Zhang, S. S. *Electrochem. Commun.* **2010**, *12*, 22–26.
(26) Wu, Y. F.; Shi, H. Y.; Yuan, L. A.; Liu, S. Q. *Chem. Commun.* **2010**, *46*, 7763–7765.
(27) Sardesai, N.; Pan, S.; Rusling, J. *Chem. Commun.* **2009**, 4968–4970.
(28) Tian, D.; Duan, C.; Wang, W.; Cui, H. *Biosens. Bioelectron.* **2010**, *25*, 2290–2295.
(29) Geim, A. K.; Novoselov, K. S. *Nat. Mater.* **2007**, *6*, 183–191.
(30) Liu, Z.; Liu, Q.; Huang, Y.; Ma, Y.; Yin, S.; Zhang, X.; Sun, W.; Chen, Y. *Adv. Mater.* **2008**, *20*, 3924–3930.
(31) Lin, C. H.; Yang, H. H.; Zheng, C. L.; Chen, X.; Chen, G. N. *Angew. Chem., Int. Ed.* **2009**, *48*, 4785–4787.
(32) Yang, W. R.; Ratinac, K. R.; Ringer, S. P.; Thordarson, P.; Gooding, J. J.; Braet, F. *Angew. Chem., Int. Ed.* **2010**, *49*, 2114–2138.
(33) Wang, X.; Wang, C.; Qu, K.; Song, Y.; Ren, J.; Miyoshi, D.; Sugimoto, N.; Qu, X. *Adv. Funct. Mater.* **2010**, *20*, 3967–3971.
(34) Shao, Y. Y.; Wang, J.; Wu, H.; Liu, J.; Aksay, I. A.; Lin, Y. H. *Electroanalysis* **2010**, *22*, 1027–1036.
(35) Kang, X. H.; Wang, J.; Wu, H.; Aksay, I. A.; Liu, J.; Lin, Y. H. *Biosens. Bioelectron.* **2009**, *25*, 901–905.
(36) Wu, X.; Hu, Y.; Jin, J.; Zhou, N.; Wu, P.; Zhang, H.; Cai, C. *Anal. Chem.* **2010**, *82*, 3588–3596.
(37) Tang, L. H.; Feng, H. B.; Cheng, J. S.; Li, J. H. *Chem. Commun.* **2010**, *46*, 5882–5884.
(38) Chen, D.; Tang, L. H.; Li, J. H. *Chem. Soc. Rev.* **2010**, *39*, 3157–3180.
(39) Zhou, M.; Zhai, Y.; Dong, S. *Anal. Chem.* **2009**, *81*, 5603–5613.
(40) Shan, C.; Yang, H.; Song, J.; Han, D.; Ivaska, A.; Niu, L. *Anal. Chem.* **2009**, *81*, 2378–2382.
(41) Wang, Y.; Li, Y.; Tang, L.; Lu, J.; Li, J. H. *Electrochem. Commun.* **2009**, *11*, 889–892.
(42) Tang, L.; Wang, Y.; Li, Y.; Feng, H.; Lu, J.; Li, J. H. *Adv. Funct. Mater.* **2009**, *19*, 2782–2789.
(43) Wan, Y.; Lin, Z. F.; Zhang, D.; Wang, Y.; Hou, B. *Biosens. Bioelectron.* **2011**, *26*, 1959–1964.
(44) Du, D.; Wang, L.; Shao, Y.; Wang, J.; Engelhard, M. H.; Lin, Y. *Anal. Chem.* **2011**, *83*, 746–752.
(45) Du, D.; Zou, Z.; Shin, Y.; Wang, J.; Wu, H.; Engelhard, M. H.; Liu, J.; Aksay, I. A.; Lin, Y. *Anal. Chem.* **2010**, *82*, 2989–2995.
(46) Fan, F.-R. F.; Park, S.; Zhu, Y.; Ruoff, R. S.; Bard, A. J. *J. Am. Chem. Soc.* **2008**, *131*, 937–939.
(47) Chen, X. P.; Ye, H. Z.; Wang, W. Z.; Qui, B.; Lin, Z. Y.; Chen, G. N. *Electroanalysis* **2010**, *22*, 2347–2352.
(48) Wang, K.; Liu, Q. A.; Wu, X. Y.; Guan, Q. M.; Li, H. N. *Talanta* **2010**, *82*, 372–376.
(49) Chen, X. M.; Wu, G. H.; Chen, J. M.; Jiang, Y. Q.; Chen, G. N.; Oyama, M.; Chen, X.; Wang, X. R. *Biosens. Bioelectron.* **2010**, *26*, 872–876.
(50) Li, H. J.; Chen, J. A.; Han, S.; Niu, W. X.; Liu, X. Q.; Xu, G. B. *Talanta* **2009**, *79*, 165–170.
(51) Wang, Y.; Lu, J.; Tang, L.; Chang, H.; Li, J. H. *Anal. Chem.* **2009**, *81*, 9710–9715.
(52) Lilja, H.; Ulmert, D.; Vickers, A. J. *Nat. Rev. Cancer* **2008**, *8*, 268–278.
(53) Hummers, W. S.; Offeman, R. E. *J. Am. Chem. Soc.* **1958**, *80*, 1338–1339.
(54) Sau, T. K.; Murphy, C. J. *Langmuir* **2004**, *20*, 6414–6420.
(55) Liao, H.; Hafner, J. H. *Chem. Mater.* **2005**, *17*, 4636–4641.
(56) Miao, W. *Chem. Rev.* **2008**, *108*, 2506–2553.
(57) Kulmala, S.; Ala-Kleme, T.; Kulmala, A.; Papkovsky, D.; Loikas, K. *Anal. Chem.* **1998**, *70*, 1112–1118.
(58) Cui, H.; Xu, Y.; Zhang, Z. F. *Anal. Chem.* **2004**, *76*, 4002.